Published in final edited form as:
Clin Cancer Res. 2011 November 1; 17(21): 6658–6670. doi:10.1158/1078-0432.CCR-11-0046.

Disruptive *TP53* Mutation is Associated with Aggressive Disease Characteristics in an Orthotopic Murine Model of Oral Tongue Cancer

Daisuke Sano[1,*], **Tong-Xin Xie**[1,*], **Thomas J. Ow**[1,*], **Mei Zhao**[1], **Curtis R. Pickering**[1], **Ge Zhou**[1], **Vlad C. Sandulache**[1], **David A. Wheeler**[2], **Richard A. Gibbs**[2], **Carlos Caulin**[1], and **Jeffrey N. Myers**[1,**]

[1]Department of Head and Neck Surgery, The University of Texas MD Anderson Cancer Center, Houston, Texas

[2]Human Genome Sequencing Center, Baylor College of Medicine, Houston, Texas

Abstract

Purpose—To characterize tumor growth and metastatic potential in head and neck squamous cell carcinoma (HNSCC) cell lines in an orthotopic murine model of oral tongue cancer, and to correlate *TP53* mutation status with these findings.

Experimental Design—Cells from each of 48 HNSCC cell lines were orthotopically injected into the oral tongues of nude mice. Tumor volume, cervical lymph node metastasis, and mouse survival were recorded. Direct sequencing of the *TP53* gene and western blot analysis for the p53 protein after induction with 5-fluorouracil was performed. Cell lines were categorized as either mutant *TP53* or wild-type *TP53*, and lines with *TP53* mutation were further categorized on the basis of type of mutation (disruptive or non-disruptive), and level of p53 protein expression. The behavior of tumors in these different groups was compared.

Results—The 48 HNSCC cell lines showed a wide range of behavior from highly aggressive and metastatic to no tumor formation. Mice injected with cells harboring disruptive *TP53* mutations had faster tumor growth, greater incidence of cervical lymph node metastasis, and shorter survival than mice injected with cells lacking these mutations.

Conclusions—HNSCC cell lines display a wide spectrum of behavior in an orthotopic model of oral cancer. Cell lines with disruptive *TP53* mutations are more aggressive in this system, corroborating clinical reports that have linked these mutations to poor patient outcome.

Keywords

head and neck squamous cell carcinoma; *TP53*; disruptive *TP53* mutation; cervical lymph node metastasis; orthotopic nude mouse model

**Corresponding author for proof and reprints: Jeffrey N. Myers, MD, PhD, Department of Head and Neck Surgery, Unit 1445, The University of Texas MD Anderson Cancer Center, 1515 Holcombe Blvd., Houston, TX 77030-4009 (713) 745-2667 (tel) (713) 794-4662 (fax) jmyers@mdanderson.org.
*Daisuke Sano, Tong-Xin Xie, and Thomas J. Ow contributed equally to this work.

Competing interests
The authors declare that we have no competing interests.

Introduction

Head and neck squamous cell carcinoma (HNSCC) consistently ranks among the six most frequently diagnosed cancers in the world (1). In 2010, an estimated 49,260 new head and neck cancers are expected in the United States (2). Currently, no molecular biomarkers are available to aid in decisions about treatment of HNSCC. Although human papillomavirus (HPV) infection has been associated with increased lymphatic metastasis and improved response to chemotherapy and radiation treatment (3), this finding has been associated with squamous cell carcinoma of the oropharynx, and treatment of patients with HPV-positive tumors currently remains the same as for those with HPV-negative tumors. Another candidate biomarker in HNSCC is mutation in the *TP53* gene. The *TP53* gene is frequently altered in HNSCC, reported in about 40% of cases (4–6). Several groups have shown that mutation in *TP53* correlates with poor response to therapy and shorter survival in patients with HNSCC (7–10).

In 2007, Poeta et al. evaluated the *TP53* mutation status in 420 patients with HNSCC that had been treated surgically, and correlated *TP53* mutations with clinical outcomes (7). In their study, they classified *TP53* mutation into disruptive and non-disruptive mutations, defining disruptive mutations as either nonsense mutations or missense mutations in the L2-L3 DNA binding domain of p53 leading to an amino acid change resulting in a residue with a different polarity or charge. All other mutations were classified as non-disruptive. Based upon this classification, they found that patients with tumors containing mutant p53 were associated with decreased survival compared to those with p53 wild-type tumors, and that disruptive mutations were associated with the shortest survival. The study by Poeta et al. provides clinical evidence that disruptive *TP53* mutation is prognostic for poor outcome in patients treated surgically for HNSCC. Despite strong evidence that disruptive *TP53* mutation is associated with worse outcome in patients with HNSCC, it remains unclear whether disruptive *TP53* mutations are associated with tumors with more aggressive tumor growth and metastasis specifically. Therefore, we evaluated the association of *TP53* mutations in a panel of HNSCC cell lines with outcomes after these cell lines were assessed in an orthotopic murine xenograft model in the present study.

Preclinical animal xenograft tumor models are widely used to study the growth and spread of cancer as well as to examine the therapeutic efficacy and mechanisms of action of new antitumor agents. Orthotopic animal models have been useful in advancing our understanding of the mechanisms of regional and distant metastatic spread of HNSCC (11), because the implantation of tumor cells into the anatomical site of tumor origin rather than into subcutaneous or other heterotopic implantation sites more closely resembles the host microenvironments present in the clinical setting of HNSCC (12). The orthotopic model has been previously validated, and several HNSCC cell lines have been shown to exhibit tumor invasion and cervical lymph node metastasis which are characteristic of the clinical disease (11). For decades, many groups have used the orthotopic xenograft system to study HNSCC, but most have evaluated 1 or 2 cell lines alone to represent a clinical disease that has very heterogeneous behavior and response to treatment (13–16). A large panel of tumor cell lines should better represent the wide variability in behavior of tumors found in patients with a given cancer, leading to more widely applicable conclusions especially in the study of *TP53*, as the number and type of *TP53* mutations is large as the IARC has reported (17).

In this study, our objective was to characterize the *in vivo* behavior of 48 established HNSCC cell lines in an orthotopic xenograft nude mouse model. We characterized the baseline tumorigenic potential of a large panel of authenticated, short tandem repeat (STR) genotyped HNSCC cell lines to determine whether different cell lines of the same tumor histology exhibit a wide spectrum of tumorigenicity and metastatic potential in the

orthotopic model, mirroring the variation in tumor behavior observed clinically. We also sequenced the *TP53* gene in each of these cell lines to assess whether *TP53* mutations were associated with aggressive tumor behavior in the *in vivo* model, matching previously reported clinical observations.

Materials and Methods

Animals and maintenance

Male athymic nude mice, ages 8–12 weeks, were purchased from the animal production area of the National Cancer Institute-Frederick Cancer Research and Development Center (Frederick, MD). The mice were housed and maintained in laminar flow cabinets under specific pathogen-free conditions. The facilities were approved by the Association for Assessment and Accreditation of Laboratory Animal Care International in accordance with current regulations and standards of the U.S. Department of Agriculture, the US Department of Health and Human Services, and the National Institute of Health. The mice were used in accordance with the Animal Care and Use Guidelines of The University of Texas MD Anderson Cancer Center under a protocol approved by the Institutional Animal Care and Use Committee.

Cell lines and culture conditions

We evaluated 48 HNSCC cell lines. Information about each cell line and appropriate growth media is shown in Supplementary Table S1. Adherent monolayer cultures were maintained on plastic and incubated at 37°C in 5% CO_2 and 95% air. The integrity of all maintained cell lines was clearly established using STR profiling. The integrity of each maintained cell line was clearly established by comparing the result from STR profiling (18) with that reported for the original stock. The cultures were free of *Mycoplasma* species and were maintained for no longer than 12 weeks after recovery from frozen stocks.

Orthotopic nude mouse model of HNSCC

To determine the tumorigenicity and metastatic potential of the 48 HNSCC cell lines, we used the orthotopic nude mouse model of HNSCC (11, 12). Each of the HNSCC cell lines was harvested from subconfluent cultures by trypsinization and washed. HNSCC cells (5×10^4 cells suspended in 30 μL of serum-free medium) were injected into the lateral tongue as described previously (11). For each cell line, 8–10 mice were prepared. Twice a week, the mice were weighed to determine weight loss and the tumor was measured in 2 dimensions with microcalipers. Tumor volume was calculated as $V = AB^2(\pi/6)$, where A is the longest dimension of the tumor and B is the dimension of the tumor perpendicular to A. The mice were asphyxiated with CO_2 when they had lost more than 20% of their pre-injection body weight or had become moribund. The remaining mice were asphyxiated 60 days after cell injection.

At necropsy, the tongue tumors and cervical lymph nodes were removed. Each tumor was fixed in formalin and embedded in paraffin for immunohistochemistry and hematoxylin and eosin (H&E) staining. The cervical lymph nodes were also embedded in paraffin and sectioned, stained with H&E, and evaluated for metastasis by light microscopy. Each lymph node identified was evaluated by H&N staining of a single cross-section through the lymph node. Measurement of tumor volume on day 32 was chosen for comparative purposes to determine the tumorigenicity of cell lines, as it was found that the majority of aggressive cell lines established modest tumors by this date.

Direct sequencing of *TP53*

Sequencing of *TP53* was performed on all 48 HNSCC cell lines. Cells from each line were cultured, trypsinized, and pelleted via centrifugation. Genomic DNA was then extracted with the QIAamp DNA Mini Kit (QIAGEN, Germantown, MD), and exons 2–11 of coding regions and splice sites of the *TP53* gene were evaluated via direct sequencing. Sequencing was performed twice for each cell line, once at the Baylor College of Medicine Human Genome Sequencing Center and once through the sequencing service provided by Beckman Coulter Genomics (Brea, CA). When there was a discrepancy between the 2 sequencing results, the tracings were reviewed to arrive at the final sequencing result.

Western blotting

We performed western blot analyses to determine expression of p53 in each HNSCC cell line. Cells from each of the 48 HNSCC cell lines were individually plated in 6-cm plates (Costar, Cambridge, MA) and incubated for 24 hours. The media was then changed in control plates, whereas a second plate for each cell line was treated with 5 μg/mL 5-fluorouracil (Sigma, St. Louis, MO) for 24 hours to elicit a DNA damage response and thereby amplify wild-type p53. Cells were then lysed using RIPA buffer, and the protein fraction was collected and evaluated via western blot analysis as previously described (13). The membranes were blocked for 1 hour at room temperature with 5% BSA in Tris-buffered saline containing 0.1% Tween 20 (TBS-T) and incubated overnight at 4°C with anti-p53 DO-1 (1:1000; Santa Cruz Biotechnology, CA) in 5% BSA in TBS-T. Next, the membranes were washed with TBS-T and incubated for 1 hour at room temperature in species-appropriate fluorescently conjugated secondary antibodies (goat anti-mouse IRDye 800, Invitrogen, Carlsbad, CA). The membranes were then analyzed using the SuperSignal West chemiluminescence system (Pierce Biotechnology, Rockford, IL) and an Odyssey infrared imaging system (LI-COR Biosciences, Lincoln, NE). Relevant signal intensities were determined using LI-COR imaging software version 3.0. To verify equal protein loading, the membranes were probed with anti-β-actin (1:5000).

TP53 Mutation analysis

Wild-type *TP53* was defined as unperturbed sequence of p53 DNA. Mutations were grouped into disruptive and non-disruptive categories. Disruptive mutations, as described previously (7), were defined as any mutation leading to a stop codon, or missense mutations occurring within the L2–L3 loop of the key DNA-binding domain, leading to substitution with an amino acid of a different polarity or charge group. All other mutations were defined as non-disruptive. We also applied an alternate classification system based on *TP53* mutation and p53 protein expression, combined. Null mutations were defined as p53 mutations that showed loss of p53 expression on western blot analysis in both basal and 5-fluorouracil induced conditions. Overexpressed mutations were defined as cell lines with mutant *TP53* and high basal levels of p53 expression. Overexpressed mutations were then further classified into disruptive and non-disruptive mutations, as described above.

Immunohistochemical Detection

One representative unstained slide of an orthotopic tumor from each cell line was chosen for immunohistochemical detection of p53 using CM-1 antibody (1:200; Leica Microsystems, Inc., Deerfield, IL). Immunohistochemical procedures were done as described previously (13). Immunostained slides were reviewed by two investigators (VCS and TJO) blinded to cell line and p53 status. Slides were scored for the presence of stained tumor cells, greater or less than 50% of tumor cells with positive staining, as well as nuclear and/or cytoplasmic staining. After blinded review, any discrepancies between the two reviewers were discussed between the two reviewers to arrive at a consensus.

Creation of TP53 forced-expression and p53-shRNA cell lines

To make a construct expressing mutant p53-P151S, total RNA was isolated from Tu138 cells with TRIzol reagent (Invitrogen, Carlsbad, CA) and reverse transcription PCR was performed to amplify p53 cDNA with the IscriptTM cDNA Synthesis kit (Bio-Rad, Richmond, CA) using the primers: 5′-BamH I: 5′ cgggatccaagtctagagccaccgtcca and 3′-EcoR I, 5′-GGAATTCTCAGTCTGAGTCAGGCCCTTCTGTC. The PCR products were inserted into the BamH I and EcoR I restriction sites of the pBaBe-puro retroviral vector (Addgene, Cambridge, MA). After verification of the mutant p53 by direct sequencing, the pBaBe-p53-P151S construct was transfected into Phoenix cells with two helper plasmids, pCGP and pVSVG, to generate virus. The cell culture supernatant was filtered and used to infect UM-SCC-1 cells to carry a splice-site mutation making it p53-null. The infected cells were selected with puromycin and pooled cells were used in the study.

To decrease the expression of mutant p53 in Tu138 cells, lenti-viral vector pLVUHshp53 containing shRNA that targets p53 was purchased from Addgene, along with the helper plasmids, pMD2.G and pCMV-dR8.2 dvpr. These were transfected into 293T cells. The supernatant was filtered and used to infect Tu138 cells. The infected cells were sorted with flow cytometry using the GFP selection marker expressed by pLVUHshp53.

Statistical analysis

Pearson's correlation coefficients were computed for the relationships between survival time and tumor volume on day 32 and between incidence of cervical lymph node metastasis and tumor volume on day 32, and *P* values were determined for the 2-tailed test. Survival was analyzed by the Kaplan–Meier method and compared with log-rank tests. Fisher's exact test was used to analyze associations between *TP53* mutation status and incidence of cervical lymph node metastasis. The unpaired 2-tailed *t* test was used to compare the differences in mean tumor volume between groups. Analysis was performed with GraphPad Prism version 5.01 (GraphPad Software, San Diego, CA). For all comparisons, $P < 0.05$ was considered statistically significant.

Results

Spectrum of tumorigenicity across 48 HNSCC cell lines in the orthotopic model

The mean tumor volumes that were measured twice a week after tumor cell implantation are shown in Supplementary Figure S1 for each of the 48 HNSCC cell lines. Seven cell lines (UM-SCC-11A, UM-SCC-11B, UM-SCC-19, UM-SCC-22B, UM-SCC-25, MDA1386TU, and MDA1386LN) did not form tumors in any of the mice injected. The remaining 41 (85.4%) HNSCC cell lines formed tumors in the tongues of nude mice with an incidence shown in Table 1. Survival curves for mice injected with each of the 48 HNSCC cell lines are shown in Supplementary Figure S2. The mean survival time ranged from 20.7 to 60.0 days. We found a strong inverse correlation between mean tumor volume on day 32 and mean survival time ($r = -0.969$, $P < 0.0001$) (Supplementary Figure S3A).

A subset of HNSCC cell lines produce cervical lymph node metastases in the orthotopic model

To study the metastatic potential of HNSCC cell lines in the orthotopic model, we harvested cervical lymph nodes at necropsy, and examined them histologically to identify metastases. We found that 19 (39.6%) of the 48 HNSCC cell lines produced cervical lymph node metastases (Table 1). The incidence (percentage of mice with lymph node metastasis) ranged from 0% to 88%. The HN5, HN31, FaDu, OSC-19, and Detroit562 cell lines developed metastases at the highest rate; cervical disease was identified in 50% or more of the mice injected with each of these cell lines. We found a correlation between mean tumor

volume on day 32 and incidence of cervical lymph node metastasis ($r = 0.581$, $P < 0.0001$) (Supplementary Figure S3B).

TP53 mutation status of 48 HNSCC cell lines

The *TP53* gene was analyzed in 48 HNSCC cell lines by direct sequencing of genomic DNA (Table 2). Five (10.4%) of the cell lines (HN30, UM-SCC-6, UM-SCC-17A, UM-SCC-25, and UM-SCC-47) were classified as having wild-type *TP53*, and the other 43 (89.6%) were found to have mutations in *TP53*. Eight (16.7%) of the cell lines (HN31, UM-SCC-4, MDA1686, MDA1986LN, FaDu, OSC-19, TR146, and CAL-27) were found to have disruptive *TP53* mutations. The other 35 (73.0%) were found to have non-disruptive *TP53* mutations; these included 23 missense mutations, 4 deletion mutations, and 8 mutations identified at splice sites (7) (Table 2).

Cell lines with disruptive *TP53* mutations show more aggressive tumor growth, higher rates of cervical lymph node metastasis, and are associated with shorter survival

To determine whether there was an association between tumor behavior and *TP53* mutation, we categorized mice into groups by *TP53* mutation status (wild-type, non-disruptive, or disruptive) and compared survival time between these groups using Kaplan–Meier survival analysis and log-rank tests. The mean survival times for the wild-type *TP53* group and the mutant *TP53* group were 55.1 and 51.7 days, respectively. Although mice in the wild-type *TP53* group survived longer than those in the mutant *TP53* group, this difference was not significant (hazard ratio [HR], 0.607; 95% confidence interval [CI], 0.360 to 1.025; $P = 0.061$) (Figure 1A, Table 3). We also determined whether there was an association between the mean tumor volume on day 32 and *TP53* mutation status (wild-type versus mutant) (Figure 1C). Although the mean tumor volume appeared smaller in the wild-type group than in the mutant group (9.22 mm^3 versus 16.10 mm^3), this difference was not significant ($P = 0.073$).

We found that the cell lines with disruptive *TP53* mutations were significantly more aggressive than those with wild-type *TP53* or non-disruptive *TP53* mutations. The mean survival time for mice whose tumors had disruptive *TP53* mutations was 46.2 days, significantly shorter than those for mice whose tumors had wild-type *TP53* (HR, 0.340; CI, 0.192 to 0.603; $P = 0.0002$) or non-disruptive *TP53* mutations (HR, 0.347; CI, 0.217 to 0.553; $P < 0.0001$) (Figure 1B, Table 3). However, the difference in mean survival time between the wild-type *TP53* group and the non-disruptive *TP53* mutation group (55.1 days versus 52.9 days) was not significant (HR, 0.682; CI, 0.383 to 1.214; $P = 0.193$) (Figure 1B, Table 3). The mean tumor volume on day 32 was also significantly higher in the disruptive *TP53* mutation group (26.12 mm^3) than in the wild-type *TP53* group (9.22 mm^3) and the non-disruptive *TP53* mutation group (13.83 mm^3) ($P = 0.0003$ and $P = 0.0001$, respectively) (Figure 1D).

Cervical lymph node metastasis was detected in only 1 (2.0%) of the 49 mice in the wild-type group (Table 4). In the mutant *TP53* group, 51 (12.1%) of the 421 mice developed cervical lymph node metastasis. We found that 29 (8.4%) of the 345 mice in the non-disruptive *TP53* mutation group and 22 (29.0%) of the 76 mice in the disruptive *TP53* mutation group developed cervical lymph node metastasis. Thus, mice in the disruptive *TP53* mutation group showed a significantly higher incidence of cervical lymph node metastasis than mice in the wild-type group ($P = 0.0001$) and the non-disruptive *TP53* group ($P = 0.0001$). Mice in the mutant *TP53* group also showed a significantly higher incidence of cervical lymph node metastasis than those in the wild-type group ($P = 0.030$). Although the incidence of cervical lymph node metastasis was also higher for mice in the non-

disruptive group than for those in the wild-type *TP53* group, this difference was not significant ($P = 0.152$).

Mutation analysis combined with protein expression defines a p53-null group of cell lines

We also performed western blot analyses to determine whether mutation in the *TP53* gene led to p53 protein stabilization or loss of expression (Table 2 and Supplementary Figure 4). We found that mutation in *TP53* led to overexpression and stabilization of mutant p53 protein in 29 cell lines, whereas protein expression was lost in 14 cell lines (which we refer to as null cell lines). Of the 14 null cell lines, 10 carried splice site or deletion mutations. The 14 p53-null cell lines were categorized into a separate group, and compared with the wild-type group (5 cell lines) and the overexpressed mutation group (29 cell lines). The overexpressed p53 mutation group was then stratified into non-disruptive (23 cell lines) and disruptive (6 cell lines) groups, as defined previously.

Whereas the mean survival time for the overexpressed group (50.8 days) was significantly shorter than that for the wild-type group (55.1 days) (HR, 0.583; CI, 0.342 to 0.993; $P = 0.047$), the difference between the null group (52.2 days) and the wild-type group was not significant (HR, 0.628; CI, 0.333 to 1.181; $P = 0.149$). However, after stratification of the overexpressed mutation group into disruptive and non-disruptive categories, the mean survival time for disruptive p53 mutation (46.1 days) was significantly shorter than that for the wild-type (HR, 0.306; CI, 0.161 to 0.580; $P = 0.0003$), null (HR, 2.409; CI, 1.403 to 4.138; $P = 0.0014$), and non-disruptive (HR, 0.335; CI, 0.207 to 0.609; $P = 0.0002$) groups. The difference between the mean survival time for the wild-type group and that for the non-disruptive group (52.1 days) again was not significant (HR, 0.660; CI, 0.365 to 1.194; $P = 0.169$) (Figure 2A and B, Table 3).

The mean tumor volumes on day 32 for the null group, overexpressed mutation group, and non-disruptive group were not significantly different from that for the wild-type group ($P = 0.139$, $P = 0.091$, and $P = 0.231$, respectively) (Figure 2C and 2D). However, the mean tumor volume on day 32 for the disruptive *TP53* mutation group was significantly higher than those for the wild-type *TP53*, null, and non-disruptive *TP53* mutation groups ($P = 0.0003$, $P = 0.0002$, and $P = 0.0002$, respectively) (Figure. 2D).

Cervical lymph node metastasis was detected in 12 (8.7%) of the 138 mice in the null group, 39 (13.8%) of the 283 mice in the overexpressed mutation group, 23 (10.1%) of the 227 mice in the non-disruptive group, and 16 (28.6%) of the 56 mice whose tumors had disruptive *TP53* mutations (Table 3). Thus, mice in the disruptive *TP53* mutation group showed a significantly higher incidence of cervical lymph node metastasis than those in the wild-type group, the null group, the overexpressed mutation group, and the non-disruptive mutation group ($P = 0.0001$ for all four). Although the incidence of cervical lymph node metastasis was higher for mice in the null p53 group and the non-disruptive group than for those in the wild-type *TP53* group, these differences were not significant ($P = 0.189$ for null and $P = 0.091$ for non-disruptive). The difference in incidence of cervical lymph node metastasis between the wild-type group and the overexpressed mutation *TP53* group was significant ($P = 0.016$).

Immunostaining patterns associated with *TP53* status

Thirty-eight orthotopic tumors were available for p53 immunohistochemical analysis (Supplementary Table S2 and Supplementary Figure S5). Among the four cell lines that were TP53 wildtype, three lines showed positive staining for p53, with a variable staining pattern in >50% of tumor cells present. Interestingly, UM-SCC-47, the only line among the panel which is positive for HPV DNA (19) was among these lines. UM-SCC-6 showed no

cells positive for p53. Among the 9 cell lines that were absent for p53 after immunoblotting with DO-1, 6 showed an absence of p53 expression upon immunohistochemical evaluation. HN4 and MDA686LN showed diffuse, intense staining, whereas OSC-19 showed positive staining in a variable pattern in >50% of tumor cells. Among the 26 cell lines that showed overexpression of p53 on western blot analysis, all of the tumors from these cell lines showed expression of p53, with diffuse staining in 24 of these. UM-SCC-17B and UM-SCC-22A showed some variability in p53 staining with >50% of tumor cells staining. In general, there appeared to be specific staining patterns that corresponded to *TP53* status- ie. a positive but variable pattern was associated with *TP53* wildtype status, TP53 missense mutation appeared to be associated with diffuse positive staining, and and *TP53* nonsense, deletions, and splice mutations appeared to be more often associated with the absence of staining. However, there were discrepancies as noted above.

Gain of function activity of an overexpressed p53 mutant is demonstrated in the orthotopic xenograft model

It was noted that the Tu138 cell line was highly aggressive in the orthotopic model, and this cell line harbored a relatively novel mutation, converting proline to serine at codon151. P53 was overexpressed in this cell line, and the mutation is classified as “non-disruptive” because it is outside of the L2-L3 loop. In order to test potential gain-of-function properties of the p53-p151s mutant, we orthotopically injected Tu138 lentiviral control, Tu138-lenti shp53, UM-SCC-1-pBabe, and UM-SCC-1-pBabe-p53p151s into ten nude mice for each cell line. Forced-expression of the mutant p53 in UM-SCC-1 cells resulted in enhanced tumor growth and decreased survival compared to UM-SCC-1pBabe control cells (Figure 3A and 3B), whereas, reduced p53-p151s expression in Tu138 cells led to slower tumor growth and longer survival in comparison to Tu138 empty-vector control cells (Figure 3C and 3D). Furthermore, p53-p151s conferred metastatic behavior to the UM-SCC-1 cell line, which was non-metastatic in transfected cells (Figure 3E). Similarly, decreased endogenous expression of p53-p151s in Tu138 resulted in decreased incidence of metastasis (Figure 3F and 3G).

Discussion

In this study, we determined the *in vivo* growth and metastatic characteristics of 48 HNSCC cell lines using an orthotopic xenograft nude mouse model of oral tongue carcinoma. A wide range of behavior was observed, from cell lines that formed no tumors to those that formed tumors that grew rapidly and consistently metastasized. We examined the *TP53* mutation status and tumor behavior, and showed that cell lines with disruptive *TP53* mutations were associated with shorter survival, faster tumor growth, and increased incidence of cervical lymph node metastasis in the orthotopic model of HNSCC.

Our study of 48 HNSCC cell lines in this *in vivo* model is the most comprehensive to date. We have shown that both tumor growth rate and incidence of cervical lymph node metastasis vary considerably between cell lines, consistent with the range of behavior observed clinically between tumors in individual HNSCC patients. Although we found some correlation between tumor volume and incidence of cervical lymph node metastasis, some of the cell lines with the highest rates of cervical lymph node metastasis showed only a moderate tumor volume, whereas some cell lines with fast tumor growth did not form metastases. These findings suggest that cell characteristics other than proliferation rate contribute to metastasis and that these cell lines can be differentiated by using this orthotopic model. The data presented here provide a valuable resource for future studies of HNSCC tumor progression and metastasis using the orthotopic xenograft model and HNSCC cells.

We chose to study *TP53* mutation because of the fundamental role p53 appears to play in HNSCC (20). After analyzing the *TP53* sequence of 48 HNSCC cell lines, we found that only 5 (10.4%) of the cell lines retained the wild-type *TP53* sequence; this is a substantially lower proportion than that reported in clinical specimens, which is typically 40–60% (7, 9, 21). This observation may suggest that there is a selection for *TP53* mutations when immortalized cell lines are established, or perhaps the incidence of *TP53* mutation in the clinical setting is underreported, for example as a result of the inherent contamination of tumor specimens with normal tissue containing wild-type *TP53*. This latter possibility is consistent with findings of a large scale exomic sequencing of oral cavity cancers that we are completing (our unpublished observations).

The strongest evidence to date linking *TP53* mutation with outcome in HNSCC has been presented by Poeta et al., who found that disruptive mutations were associated with decreased overall survival (7). In our study, we consistently observed that disruptive *TP53* mutations were significantly associated with shorter survival, greater tumor volume, and increased incidence of cervical lymph node metastasis in the orthotopic xenograft model. These results indicate that disruptive *TP53* mutations may play a critical role in the progression and metastasis of HNSCC and support previous clinical reports concluding that disruptive *TP53* mutations are a prognostic biomarker for patients with HNSCC.

Despite our evidence supporting the disruptive/non-disruptive classification system, it is recognized that this categorization has a theoretic structural basis which predicts p53 function based on the substituted amino acid's location and type. We have isolated the p151s mutation, classified as 'non-disruptive', and demonstrated that it has significant gain-of-function activity in our model. It is possible that the disruptive categorization merely selects for mutations that are deleterious, and it seems that a more concrete delineation of p53 mutations based on alteration of function or demonstration of one or several consistent gain-of-function mechanisms is necessary. The fact that *TP53*-null mutations were relatively benign in our study suggests that gain-of-function activity may contribute significantly to the deleterious effect of *TP53* mutations associated with the poorest outcome. A large-scale analysis of *TP53* mutations is required to identify and characterize the most deleterious mutations from a mechanistic standpoint.

In our study, we found that most of the insertion, deletion, and splice mutations resulted in loss of p53 expression. Therefore, we used the combination of mutation and lack of protein expression to further define a separate, p53 null group. Although previous clinical studies of ovarian cancer have suggested that patients with tumors containing p53 null mutations are at risk for distant metastases and have a poor prognosis (22, 23), we found that cell lines with null mutations were significantly less aggressive than those in the disruptive *TP53* category, suggesting that p53 null mutations are less deleterious than disruptive mutations in HNSCC cells.

A recent publication has reported that truncating *TP*53 mutations, defined as nonsense, splice, and frameshift mutations, and largely represented by the "null' group in our study, are associated with poor prognosis among patients with HNSCC (24). The discrepancy of our data with this literature may be due to several considerations. The most obvious is that mice in our study are not treated for their disease, whereas patients in the study by Lindenbergher et al. were treated with either surgery or surgery and post-operative radiation. It may be that specific *TP53* mutations contribute greatly to tumor formation and progression, whereas other mutations are more deleterious the setting of radiation therapy. A second consideration is that a significant number of patients in the study had oropharyngeal tumors, and though HPV was evaluated in this study, microenvironmental factors specific to the lymphoid-rich oropharynx may contribute to tumor phenotype and thus alter the role of

TP53 mutation. Further mechanistic evaluation is required, and our work represents a model in which these questions can be isolated and examined in future studies.

The categorization of mutations into disruptive and non-disruptive is not the only system that has been correlated with outcome in HNSCC. Another classification scheme has been described that is based on p53 transactivation activity in a yeast-based functional assay (6, 25). The transactivation activity of p53 plays a key role in its tumor suppressor function, and it has been shown that a genetically engineered mouse model carrying a transactivation-deficient *TP53* mutation is predisposed to cancer development (26, 27). Perrone et al. recently reported that oral cavity tumors with wild-type *TP53* or mutations that retain partial transactivation ability showed a higher response rate to induction chemotherapy (8). In the present study, 28 of the cell lines could be categorized by functional status on the basis of transactivation ability. Splice site, deletion, and mutations resulting in a premature stop codon are not classifiable by this system, although the majority would be considered non-functional. We classified these 28 cell lines into fully functional, partially functional, and nonfunctional groups. However, only 2 of the 28 cell lines carried mutations that retained partial transactivation ability, whereas all others were classified as nonfunctional. As expected, in the orthotopic nude mouse model the cell lines with nonfunctional p53 mutations were associated with shorter survival, greater tumor volume, and increased incidence of cervical lymph node metastasis than the cell lines with wild-type or partially functional p53 mutations (data not shown). Because only a few of our panel of cell lines carried mutations that retained partial transactivation ability, it is difficult to draw conclusions about the role of partially functional mutations in our system from these results. The true impact of partially functional mutations in HNSCC remains to be elucidated, and this could perhaps be further studied in the preclinical model we describe here if more cell lines with partially functional p53 mutations are identified or created.

There are some discrepancies between *TP53* mutations identified in the present study and those described in previous reports evaluating the same HNSCC cell lines (Supplementary Table S3). In the current study, all of our cell lines were received from the American Type Culture Collection or requested directly from the laboratory from which they originated, and each line was validated using STR genotyping confirmed against that obtained by the originators (19). We also sequenced *TP53* twice in independent laboratories for each line, and confirmed p53 protein expression using western blotting. The inconsistencies between our report and those previously reported may reflect the differences of the procedures to detect *TP53* status in HNSCC cells. Alternatively, these discrepancies may be the result of cell line contamination or mis-identification in the previous reports. Discrepancies among published works reporting *TP53* status in cell lines have been reviewed, and this unfortunately occurs frequently (17). Although we cannot resolve discrepancies between existing literature and our report, we attest to undertaking rigorous cell line authentification (19) and *TP53* evaluation in our study.

In summary, we have demonstrated the utility of the orthotopic xenograft model by characterizing the largest panel of HNSCC cell lines to date. Our results have corroborated clinical reports showing that disruptive *TP53* mutations correlate with aggressive tumor characteristics. Furthermore, we have proposed a new approach to classify *TP53* mutations by combining *TP53* sequence information with p53 protein expression levels. These results suggest that disruptive *TP53* mutations may play a key role in the tumor progression and cervical lymph node metastatic potential of HNSCC. Our work should help facilitate further studies examining the cellular and molecular mechanisms of *TP53* mutations in HNSCC tumor progression, metastasis, and response to therapy.

Supplementary Material

Refer to Web version on PubMed Central for supplementary material.

Acknowledgments

Grant support

This work was supported by the University of Texas MD Anderson Cancer Center PANTHEON program, NIH Specialized Program of ResearchExcellence Grant P50CA097007, RO1 DE14613 NIH, National Research Science Award Institutional Research Training Grant T32CA60374, and NIH Cancer Center Support Grant CA016672 (CCSG).

We thank Dr. Karen Muller for her critical editorial review of the manuscript.

References

1. Ferlay J, Shin HR, Bray F, Forman D, Mathers C, Parkin DM. Estimates of worldwide burden of cancer in 2008: GLOBOCAN. Int J Cancer. 2008
2. Jemal A, Siegel R, Xu J, Ward E. Cancer Statistics, 2010. CA Cancer J Clin. 2010
3. Ang KK, Harris J, Wheeler R, Weber R, Rosenthal DI, Nguyen-Tan PF, et al. Human papillomavirus and survival of patients with oropharyngeal cancer. N Engl J Med. 2010; 363:24–35. [PubMed: 20530316]
4. Somers KD, Merrick MA, Lopez ME, Incognito LS, Schechter GL, Casey G. Frequent p53 mutations in head and neck cancer. Cancer Res. 1992; 52:5997–6000. [PubMed: 1394225]
5. Sidransky D. Emerging molecular markers of cancer. Nat Rev Cancer. 2002; 2:210–9. [PubMed: 11990857]
6. Petitjean A, Mathe E, Kato S, Ishioka C, Tavtigian SV, Hainaut P, et al. Impact of mutant p53 functional properties on TP53 mutation patterns and tumor phenotype: lessons from recent developments in the IARC TP53 database. Hum Mutat. 2007; 28:622–9. [PubMed: 17311302]
7. Poeta ML, Manola J, Goldwasser MA, Forastiere A, Benoit N, Califano JA, et al. TP53 mutations and survival in squamous-cell carcinoma of the head and neck. N Engl J Med. 2007; 357:2552–61. [PubMed: 18094376]
8. Perrone F, Bossi P, Cortelazzi B, Locati L, Quattrone P, Pierotti MA, et al. TP53 mutations and pathologic complete response to neoadjuvant cisplatin and fluorouracil chemotherapy in resected oral cavity squamous cell carcinoma. J Clin Oncol. 2010; 28:761–6. [PubMed: 20048189]
9. Temam S, Flahault A, Perie S, Monceaux G, Coulet F, Callard P, et al. p53 gene status as a predictor of tumor response to induction chemotherapy of patients with locoregionally advanced squamous cell carcinomas of the head and neck. J Clin Oncol. 2000; 18:385–94. [PubMed: 10637254]
10. Cabelguenne A, Blons H, de Waziers I, Carnot F, Houllier AM, Soussi T, et al. p53 alterations predict tumor response to neoadjuvant chemotherapy in head and neck squamous cell carcinoma: a prospective series. J Clin Oncol. 2000; 18:1465–73. [PubMed: 10735894]
11. Myers JN, Holsinger FC, Jasser SA, Bekele BN, Fidler IJ. An orthotopic nude mouse model of oral tongue squamous cell carcinoma. Clin Cancer Res. 2002; 8:293–8. [PubMed: 11801572]
12. Sano D, Myers JN. Xenograft models of head and neck cancers. Head Neck Oncol. 2009; 1:32. [PubMed: 19678942]
13. Yigitbasi OG, Younes MN, Doan D, Jasser SA, Schiff BA, Bucana CD, et al. Tumor cell and endothelial cell therapy of oral cancer by dual tyrosine kinase receptor blockade. Cancer Res. 2004; 64:7977–84. [PubMed: 15520205]
14. Yoon Y, Liang Z, Zhang X, Choe M, Zhu A, Cho HT, et al. CXC chemokine receptor-4 antagonist blocks both growth of primary tumor and metastasis of head and neck cancer in xenograft mouse models. Cancer Res. 2007; 67:7518–24. [PubMed: 17671223]

15. Zhang H, Su L, Muller S, Tighiouart M, Xu Z, Zhang X, et al. Restoration of caveolin-1 expression suppresses growth and metastasis of head and neck squamous cell carcinoma. Br J Cancer. 2008; 99:1684–94. [PubMed: 19002186]

16. Sano D, Fooshee DR, Zhao M, Andrews GA, Frederick MJ, Galer C, et al. Targeted molecular therapy of head and neck squamous cell carcinoma with the tyrosine kinase inhibitor vandetanib in a mouse model. Head Neck. 2010

17. Berglind H, Pawitan Y, Kato S, Ishioka C, Soussi T. Analysis of p53 mutation status in human cancer cell lines: a paradigm for cell line cross-contamination. Cancer Biol Ther. 2008; 7:699–708. [PubMed: 18277095]

18. Masters JR, Thomson JA, Daly-Burns B, Reid YA, Dirks WG, Packer P, et al. Short tandem repeat profiling provides an international reference standard for human cell lines. Proc Natl Acad Sci U S A. 2001; 98:8012–7. [PubMed: 11416159]

19. Zhao, M.; Sano, D.; Pickering, C.; Jasser, SA.; Henderson, YC.; Clayman, GL., et al. Assembly And Initial Characterization Of A Panel Of 85 Genomically Validated Cell Lines From Diverse Head And Neck Tumor Sites. manuscript under review

20. Forastiere A, Koch W, Trotti A, Sidransky D. Head and neck cancer. N Engl J Med. 2001; 345:1890–900. [PubMed: 11756581]

21. Koch WM, Brennan JA, Zahurak M, Goodman SN, Westra WH, Schwab D, et al. p53 mutation and locoregional treatment failure in head and neck squamous cell carcinoma. J Natl Cancer Inst. 1996; 88:1580–6. [PubMed: 8901856]

22. Sood AK, Sorosky JI, Dolan M, Anderson B, Buller RE. Distant metastases in ovarian cancer: association with p53 mutations. Clin Cancer Res. 1999; 5:2485–90. [PubMed: 10499623]

23. Rose SL, Robertson AD, Goodheart MJ, Smith BJ, DeYoung BR, Buller RE. The impact of p53 protein core domain structural alteration on ovarian cancer survival. Clin Cancer Res. 2003; 9:4139–44. [PubMed: 14519637]

24. Lindenbergh-van der Plas M, Brakenhoff RH, Kuik D, Buijze M, Bloemena E, Snijders P, et al. Prognostic significance of truncating TP53 mutations in head and neck squamous cell carcinoma. Clin Cancer Res. 2011

25. Kato S, Han SY, Liu W, Otsuka K, Shibata H, Kanamaru R, et al. Understanding the function-structure and function-mutation relationships of p53 tumor suppressor protein by high-resolution missense mutation analysis. Proc Natl Acad Sci U S A. 2003; 100:8424–9. [PubMed: 12826609]

26. Jimenez GS, Nister M, Stommel JM, Beeche M, Barcarse EA, Zhang XQ, et al. A transactivation-deficient mouse model provides insights into Trp53 regulation and function. Nat Genet. 2000; 26:37–43. [PubMed: 10973245]

27. Jacks T, Remington L, Williams BO, Schmitt EM, Halachmi S, Bronson RT, et al. Tumor spectrum analysis in p53-mutant mice. Curr Biol. 1994; 4:1–7. [PubMed: 7922305]

Statement of Translational Relevance

In vivo models of human disease and cell lines derived from patient tumors are frequently used to study cancer. Studies focusing on few cell lines using models that deviate significantly from the clinical disease can yield misleading results. Here, we provide a comprehensive review of 48 head and neck squamous cell cancer (HNSCC) cell lines evaluated in an orthotopic model of oral tongue cancer in nude mice. To demonstrate the applicability of this model to study the impact of specific biomarkers of HNSCC, we determined the *TP53* mutation status of each cell line and demonstrated that tumor behavior in this system correlates with *TP53* mutation status, supporting clinical studies reported in the literature. These data provide support for the utility of this model system for characterizing the mechanism of disease progression in HNSCC, and provide baseline data that can be utilized for pre-clinical evaluation of new therapies for HNSCC.

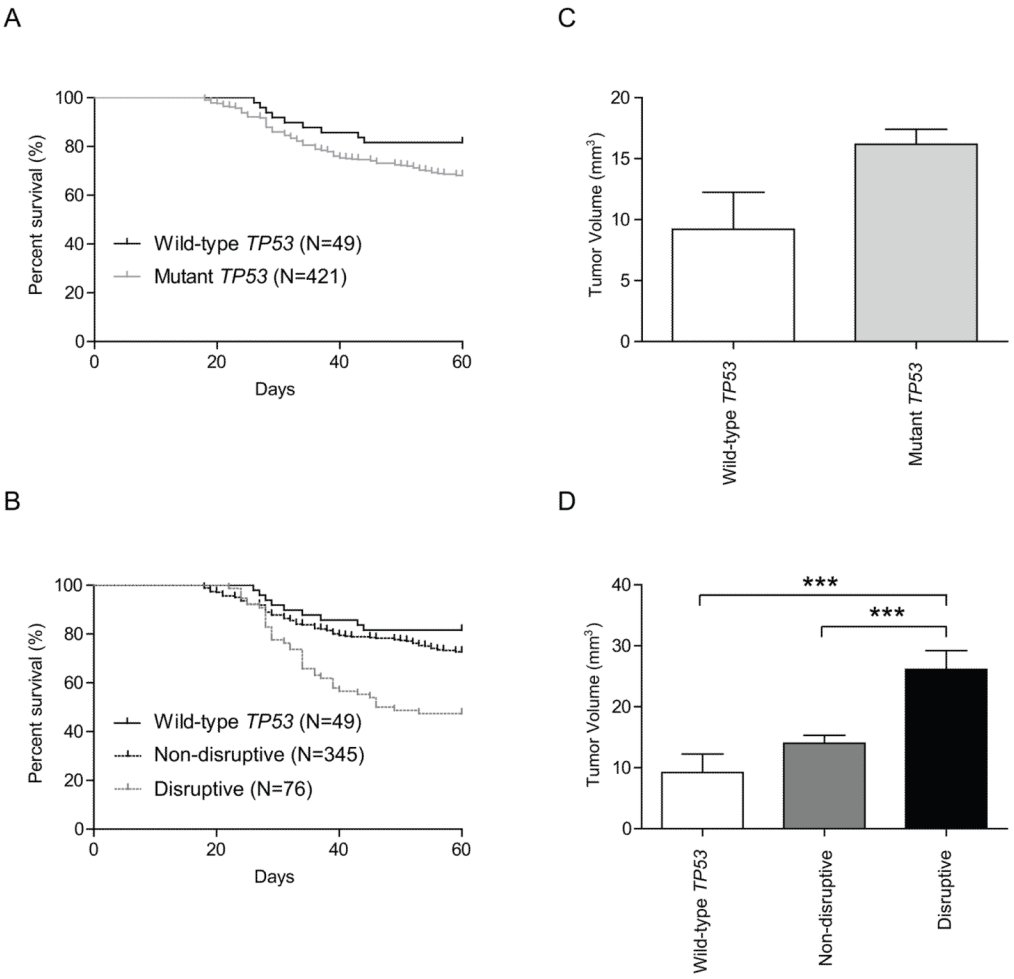

Figure 1.

Survival time and tumor volume according to *TP53* mutation status in the orthotopic nude mouse model of HNSCC. (A) Survival of wild-type group and mutant *TP53* group. (B) Survival of wild-type group, disruptive *TP53* mutations group, and non-disruptive *TP53* mutations group. Disruptive mutations were defined as either stop codon mutations in any region or missense mutations in the L2–L3 binding domain of p53 that cause an amino acid change to a residue with a different polarity or charge; All other mutations were defined as non-disruptive. (C) The mutant *TP53* group showed increased tumor volumes than wild-type *TP53* group, however, the difference did not reach statistical significant. (D) Disruptive *TP53* mutations group showed increased tumor volumes compared with both wild-type *TP53* group and non-disruptive *TP53* mutations group. Animals were asphyxiated when they had lost more than 20% of their initial body weight or had become moribund, and the remaining mice were asphyxiated 60 days after cell injection. Survival was analyzed by the Kaplan–Meier method and compared with log-rank tests. Columns, mean tumor volume; bars, standard error. ***, $P < 0.001$.

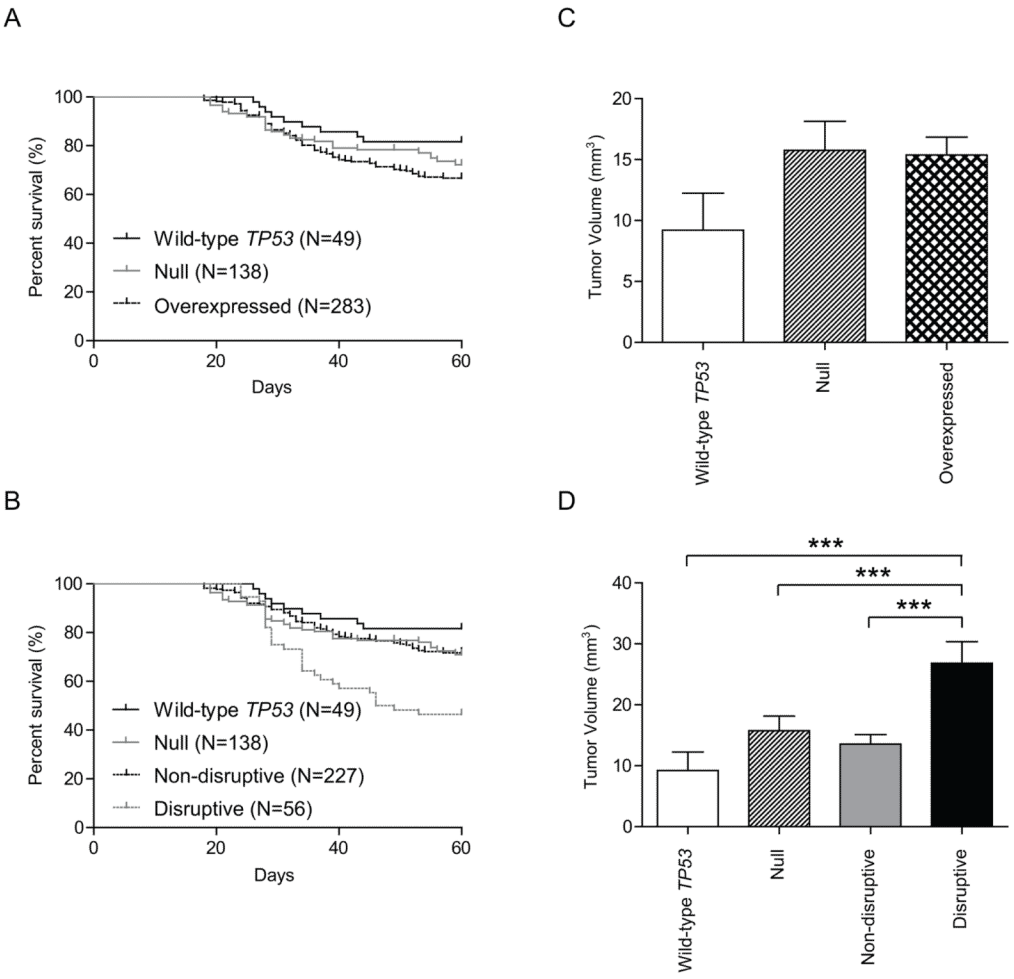

Figure 2.

Survival time and tumor volume in the orthotopic xenograft model according to *TP53* mutation status and level of p53 protein expression. (A) Survival of wild-type group, null group, and overexpressed mutation group. (B) Survival of wild-type group, null group, disruptive *TP53* mutations group, and non-disruptive *TP53* mutations group. Overexpressed mutations were defined as *TP53* mutations that lead to constitutive overexpression of p53 on western blot analysis. Null mutations were defined as *TP53* mutations that showed absence and no induction of p53 expression on western blot analysis. Overexpressed mutations were also grouped into disruptive and non-disruptive categories, as described above. (C) Both the null and overexpressed mutation groups showed increased tumor volumes as compared to the wild-type group, however, the differences did not reach statistical significance. (D) The disruptive *TP53* mutation group showed increased tumor volumes compared to the wild-type group, null group, and non-disruptive *TP53* mutation group. Animals were asphyxiated when they had lost more than 20% of their initial body weight or had become moribund, and the remaining mice were asphyxiated 60 days after cell injection. Survival was analyzed by the Kaplan Meier method and compared with log-rank tests. Columns, mean tumor volume; bars, standard error. ***, $P < 0.001$.

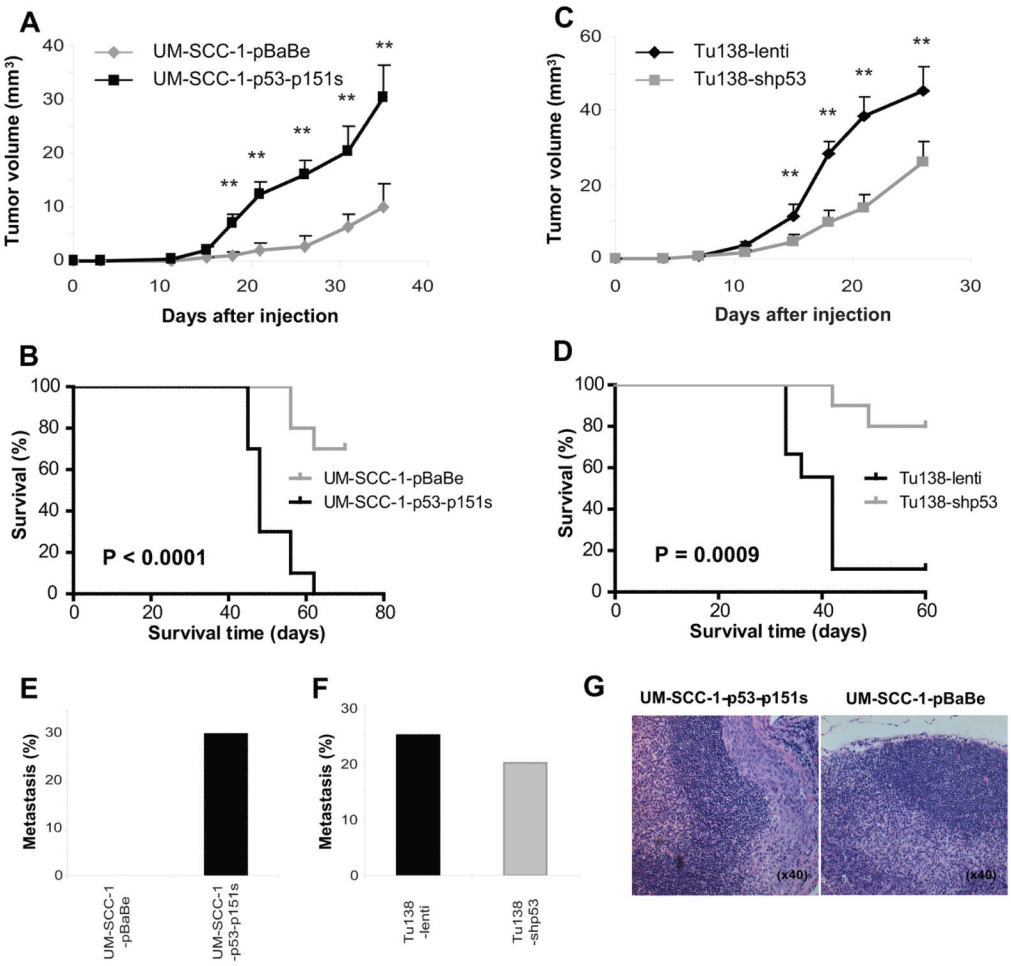

Figure 3.

The mutant p53-p151s promotes tumor progression and metastasis in a nude mouse orthotopic model. The stable UM-SCC-1-p53-p151s, Tu138-shp53 cells and their control cells were injected into the tongues of nude mice and tumor size and body weight was measured two times a week. A-F, the tumor growth, mouse survival and cervical lymph node metastasis were compared between UM-SCC-1-p53-p151s cells and their control cells (A, B, and E. **, $p<0.01$) and Tu138-shp53 and their control cells (C, D and F. **, $p<0.01$). G, Hematoxyilin and eosin slides of cervical lymph node of UM-SCC-1-p53-p151s tumor (left) and its control (right). Magnification, ×40.

Table 1

Incidence of tumor formation, tumor volume on day 32, incidence of cervical lymph node metastasis, and survival time for 48 different cell lines in the orthotopic nude mouse model of HNSCC

Cell line	Tumor formation % of mice	Tumor volume on day 32 (mm^3) * Mean ± SD	Cervical lymph node metastasis % of mice	Survival time (days) Mean ± SD
HN4	78	2.2 ± 0.4	14	59.6 ± 1.3
HN5	100	53.8 ± 5.6	50	28.2 ± 3.1
HN30	60	0.0	0	60.0
HN31	100	60.1 ± 4.9	56	28.7 ± 5.3
UM-SCC-1	90	2.0 ± 0.5	11	58.9 ± 3.5
UM-SCC-4	50	1.3 ± 0.1	0	60.0
UM-SCC-6	10	0.0	0	60.0
UM-SCC-10A	60	2.9 ± 0.6	0	60.0
UM-SCC-10B	20	1.1 ± 0.0	0	60.0
UM-SCC-11A	0	0.0	0	60.0
UM-SCC-11B	0	0.0	0	60.0
UM-SCC-14A	40	0.0	0	60.0
UM-SCC-14B	70	0.0	14	60.0
UM-SCC-17A	20	0.0	0	60.0
UM-SCC-17B	100	47.4 ± 3.1	30	25.9 ± 11.1
UM-SCC-19	0	0.0	0	60.0
UM-SCC-22A	100	52.9 ± 5.4	10	36.7 ± 8.7
UM-SCC-22B	0	0.0	0	60.0
UM-SCC-25	0	0.0	0	60.0
UM-SCC-47	100	52.6 ± 6.3	10	33.2 ± 6.8
JHU011	40	0.9 ± 0.0	0	60.0
JHU022	100	74.1 ± 4.7	20	20.7 ± 2.8
JHU029	60	2.7 ± 0.7	0	60.0
MDA686TU	90	8.6 ± 3.8	0	58.0 ± 4.2
MDA686LN	100	76.7 ± 2.7	0	28.4 ± 1.1
MDA886LN	100	2.3 ± 0.3	10	59.3 ± 2.2
MDA1186	90	13.9 ± 3.8	0	57.2 ± 4.2
MDA1386TU	0	0.0	0	60.0
MDA1386LN	0	0.0	0	60.0
MDA1586	100	4.0 ± 0.8	20	60.0
MDA1686	30	0.0	0	60.0
MDA1986LN	90	3.2 ± 1.0	0	60.0
PCI-13	70	2.6 ± 0.0	0	60.0
PCI-15A	30	1.6 ± 0.2	0	60.0
PCI-15B	70	0.0	0	60.0
PCI-24	10	0.0	0	60.0
FaDu	80	29.5 ± 3.5	88	44.3 ± 11.0
OSC-19	100	47.7 ± 7.7	60	32.7 ± 6.9

Cell line	Tumor formation % of mice	Tumor volume on day 32 (mm^3) * Mean ± SD	Cervical lymph node metastasis % of mice	Survival time (days) Mean ± SD
TR146	100	55.5 ± 5.8	33	30.9 ± 3.4
TU-138	100	50.5 ± 6.2	30	39.8 ± 11.4
SqCC/Y1	100	22.1 ± 3.3	10	50.5 ± 10.8
SCC-61	100	58.0 ± 10.2	10	27.4 ± 5.0
CAL-27	100	44.4 ± 7.5	13	49.1 ± 11.8
PE/CA-PJ34	100	8.5 ± 2.0	0	58.5 ± 4.7
Detroit562	90	50.4 ± 5.6	78	40.2 ± 11.9
183	90	10.0 ± 1.6	0	60.0
1483	70	5.5 ± 1.7	0	55.9 ± 7.0
584A2	44	0.0	0	60.0

* The data at the endpoint were used if the mouse was asphyxiated before day 32.

Abbreviation: SD, standard deviation.

Table 2

TP53 Mutation status of 48 different cell lines in the orthotopic nude mouse model of HNSCC

						p53 Protein status		
Cell line	**Mutation type**	**Codon**	**From**	**To**	**Classification of Poeta et al.**	**Baseline**	**After 5FU treatment**	**New classification**
HN4	Splice site				ND	−	−	Null
HN5	Missense	238	Cys	Ser	ND	++	++	Overexpressed, ND
HN30	Wild-type					+	++	Wild-type
HN31	Missense	176	Cys	Phe	D	++	++	Overexpressed, D
	Missense	161	Ala	Ser				
UM-SCC-1	Splice site				ND	−	−	Null
UM-SCC-4	Missense	213	Arg	STP	D	−	−	Null
UM-SCC-6	Wild-type					−	−	Wild-type
UM-SCC-10A	Missense	245	Gly	Cys	ND	++	++	Overexpressed, ND
UM-SCC-10B	Missense	390	Pro	Ser	ND	++	++	Overexpressed, ND
	Missense	245	Gly	Cys				
UM-SCC-11A	Missense	242	Cys	Ser	ND	++	++	Overexpressed, ND
UM-SCC-11B	Missense	242	Cys	Ser	ND	++	++	Overexpressed, ND
UM-SCC-14A	Deletion				ND	++	++	Overexpressed, ND
UM-SCC-14B	Deletion				ND	++	++	Overexpressed, ND
UM-SCC-17A	Wild-type					+	++	Wild-type
UM-SCC-17B	Missense	273	Arg	Cys	ND	++	++	Overexpressed, ND
UM-SCC-19	Deletion				ND	−	−	Null
UM-SCC-22A	Missense	220	Tyr	Cys	ND	++	++	Overexpressed, ND
UM-SCC-22B	Missense	220	Tyr	Cys	ND	++	++	Overexpressed, ND
UM-SCC-25	Wild-type					−	−	Wild-type
UM-SCC-47	Wild-type					+	+	Wild-type
JHU011	Splice site				ND	−	−	Null
	Missense	36	Pro	Pro				
JHU022	Splice site				ND	−	−	Null
JHU029	Splice site				ND	−	−	Null
MDA686TU	Missense	151	Pro	Ser	ND	++	++	Overexpressed, ND
MDA686LN	Missense	151	Pro	Ser	ND	−	−	Null

Cell line	Mutation type	Codon	From	To	Classification of Poeta et al.	p53 Protein status		New classification
						Baseline	After 5FU treatment	
MDA886LN	Splice site				ND	−	−	Null
MDA1186	Missense	258	Glu	Gly	ND	++	++	Overexpressed, ND
MDA1386TU	Missense	282	Arg	Trp	ND	++	++	Overexpressed, ND
MDA1386LN	Missense	282	Arg	Trp	ND	++	++	Overexpressed, ND
MDA1586	Missense	273	Arg	Leu	ND	++	++	Overexpressed, ND
MDA1686	Missense	176	Cys	Phe	D	++	++	Overexpressed, D
	Missense	218	Val	Gly				
MDA1986LN	Missense	336	Glu	STP	D	++	++	Overexpressed, D
PCI-13	Deletion				ND	−	−	Null
	Missense	356	Gly	Gly				
PCI-15A	Missense	273	Arg	Cys	ND	++	++	Overexpressed, ND
PCI-15B	Missense	273	Arg	Cys	ND	++	++	Overexpressed, ND
PCI-24	Missense	266	Gly	Arg	ND	++	++	Overexpressed, ND
FaDu	Missense	248	Arg	Leu	D	++	++	Overexpressed, D
	Deletion							
OSC-19	Missense	164	Lys	STP	D	−	−	Null
	Splice site							
TR146	Missense	248	Arg	Gln	D	++	++	Overexpressed, D
TU-138	Missense	151	Pro	Ser	ND	++	++	Overexpressed, ND
SqCC/Y1	Missense	176	Cys	Ser	ND	−	−	Null
	Missense	142	Pro	His				
SCC-61	Missense	110	Arg	Leu	ND	++	++	Overexpressed, ND
CAL-27	Missense	193	His	Leu	D	++	++	Overexpressed, D
PE/CA-PJ34	Missense	159	Ala	Val	ND	++	++	Overexpressed, ND
Detroit562	Missense	175	Arg	His	ND	++	++	Overexpressed, ND
183	Splice site				ND	−	−	Null
1483	Missense	126	Tyr	Cys	ND	++	++	Overexpressed, ND
584A2	Splice site				ND	−	−	Null

Abbreviations: 5FU, 5-fluorouracil; D, disruptive *TP53* mutation; ND, nondisruptive *TP53* mutation;

−, no expression of p53 protein;

+, expression of p53 protein;

++, overexpression of p53 protein.

Table 3

Association of *TP53* mutation status with survival time and incidence of cervical lymph node metastasis in the orthotopic nude mouse model of HNSCC

Mutation status	No. of mice	No. of deaths	Survival time (days) Mean ± SD	Hazard ratio for death (95% CI)	P value from log-rank test (verses wild-type)	No. of mice with and without cervical lymph node metastasis		% of mice with cervical lymph node metastasis	P value from Fisher's exact test (versus wild-type)
						With	Without		
p53 status									
Wild-type	49	9	55.1 ± 10.8			1	48	2	
Mutant	421	134	51.7 ± 13.5	0.6069 (0.3595 to 1.025)	0.062	51	370	12.1	0.03
Mutation category									
Classification of Poeta et al.									
Wild-type	49	9	55.1 ± 10.8			1	48	2	
Nondisruptive	345	94	52.9 ± 13.0	0.6821 (0.3832 to 1.214)	0.193	29	316	8.4	0.152
Disruptive	76	40	46.2 ± 14.4	0.340 (0.192 to 0.603)	0.0002	22	54	29	0.0001
new classification									
Wild-type	49	9	55.1 ± 10.8			1	48	2	
Null	138	40	52.2 ± 13.9	0.6275 (0.3333 to 1.181)	0.149	12	126	8.7	0.189
Overexpressed	283	94	50.8 ± 13.6	0.583 (0.342 to 0.993)	0.047	39	244	13.8	0.016
Nondisruptive	227	64	52.1 ± 13.2	0.660 (0.365 to 1.194)	0.169	23	204	10.1	0.091
Disruptive	56	30	46.1 ± 14.3	0.306 (0.161 to 0.580)	0.0003	16	40	28.6	0.0001

Abbreviation: SD, standard deviation.